Supplementary Information

Cooperation of stereo effect and host-guest interactions towards electrochemical detection of dopamine

Xiaowen Wang,[a] Xing-Yue He,[a] Ziqing Zhang,[a] Zhizeng Ni,[a] Xiao-Hang Qiu,*[a] Jian-Gong Ma,*[a] and Peng Cheng[a]

[a.] Department of Chemistry, Key Laboratory of Advanced Energy Material Chemistry (MOE), Frontiers Science Center for New Organic Matter, and Renewable Energy Conversion and Storage Center (RECAST), College of Chemistry, Nankai University, Tianjin 300071, P. R. China

Corresponding E-mail: qiuxh@nankai.edu.cn; mvbasten@nankai.edu.cn

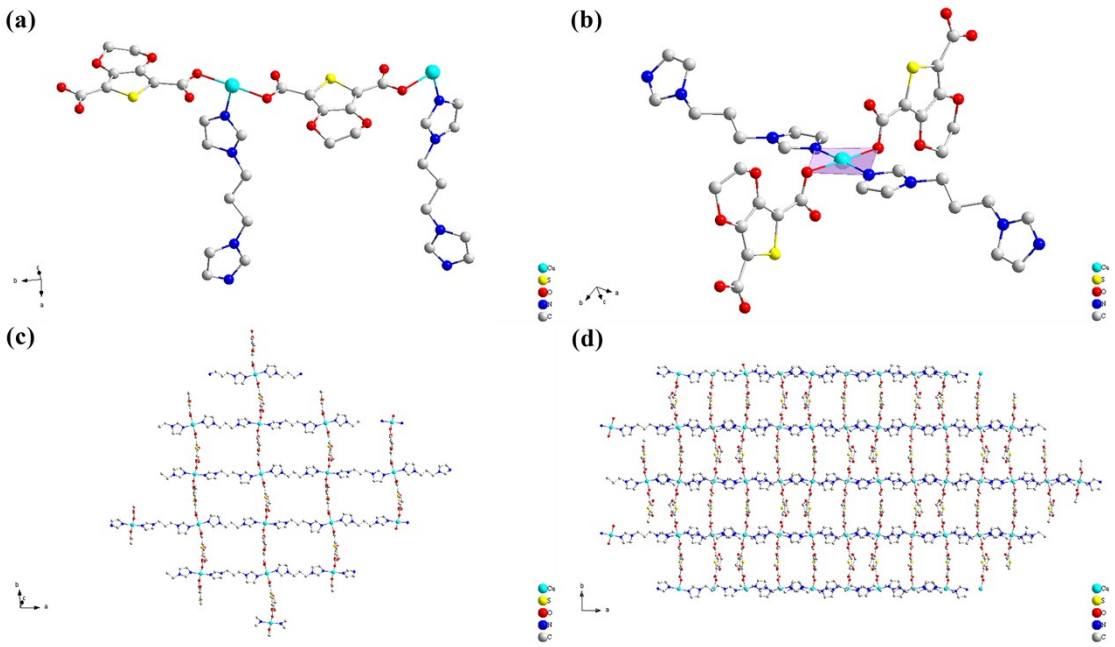

Fig. S1 Structure of Cu-MOF-3C: (a) asymmetric unit; (b) coordination environment of Cu^{2+}; (c) 2D framework; (d) 3D framework.

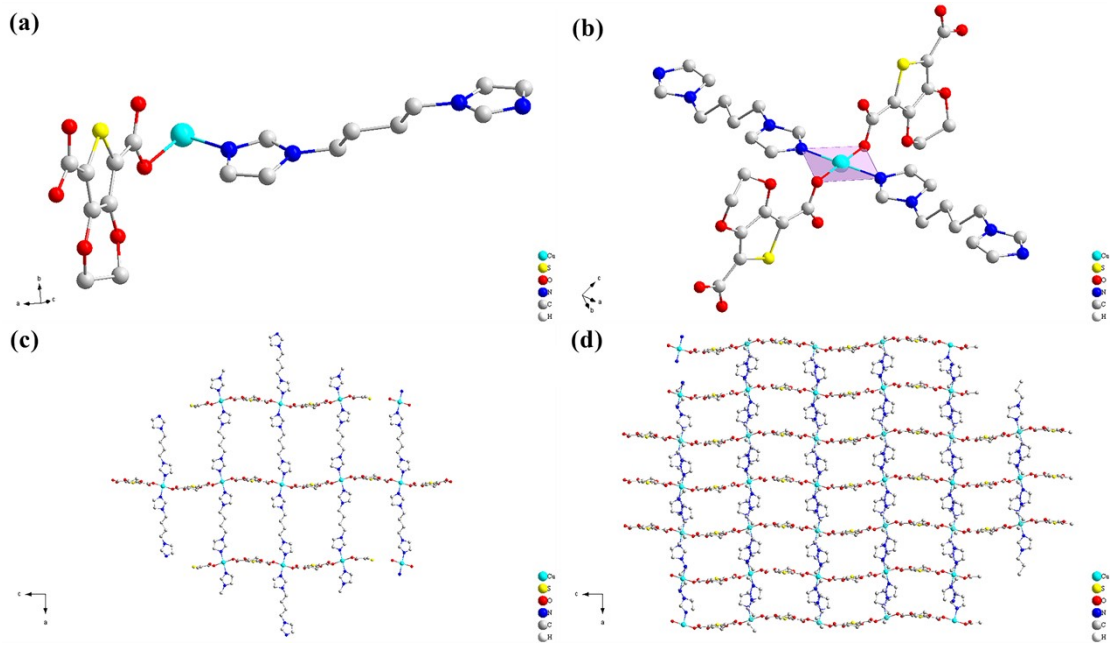

Fig. S2 Structure of Cu-MOF-4C: (a) asymmetric unit; (b) coordination environment of Cu^{2+}; (c) 2D framework; (d) 3D framework.

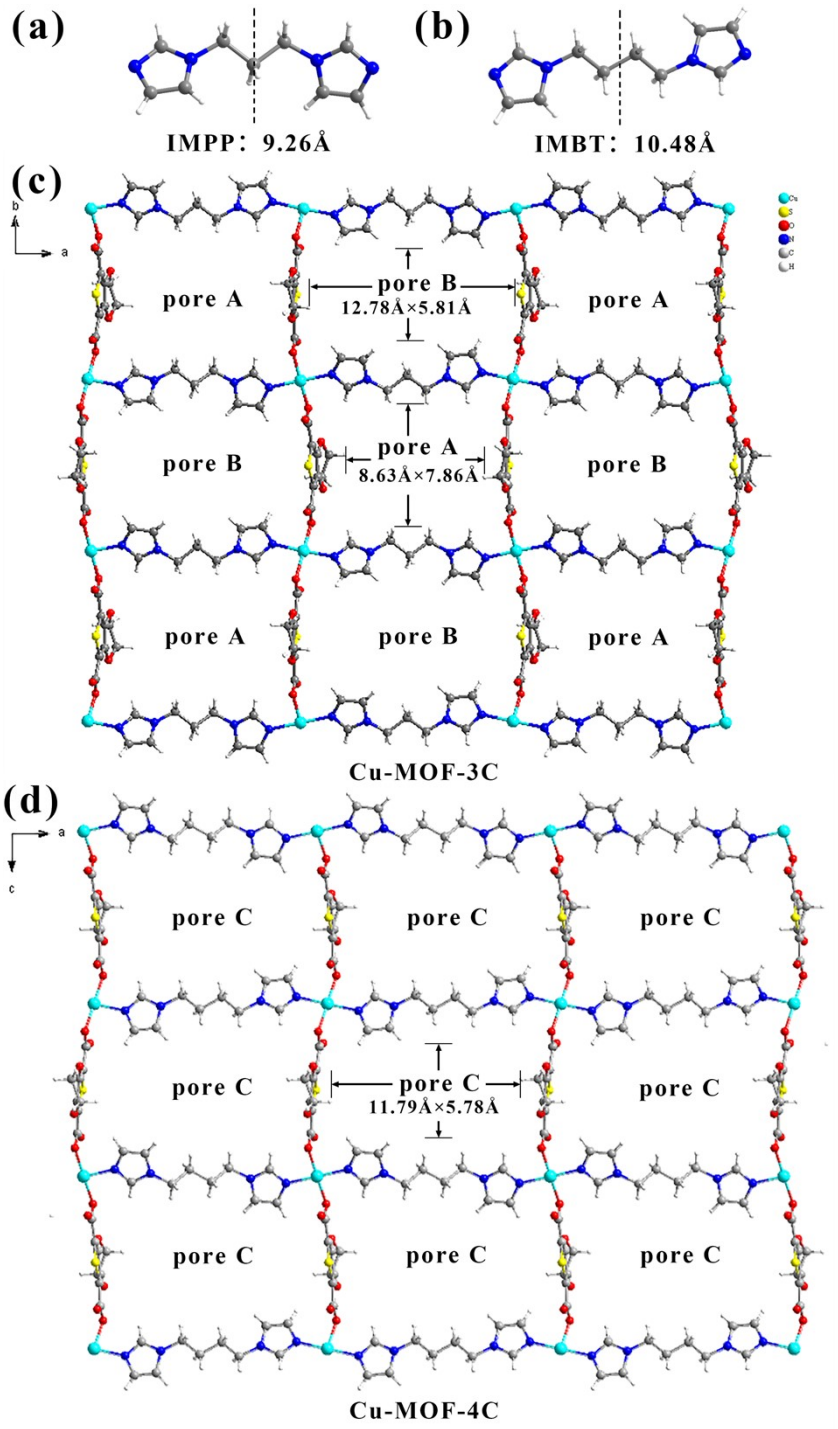

Fig. S3 The length and symmetrical patterns of ligands (a) IMPP and (b) IMBT. The intralayer pores of (b) Cu-MOF-3C and (c) Cu-MOF-4C.

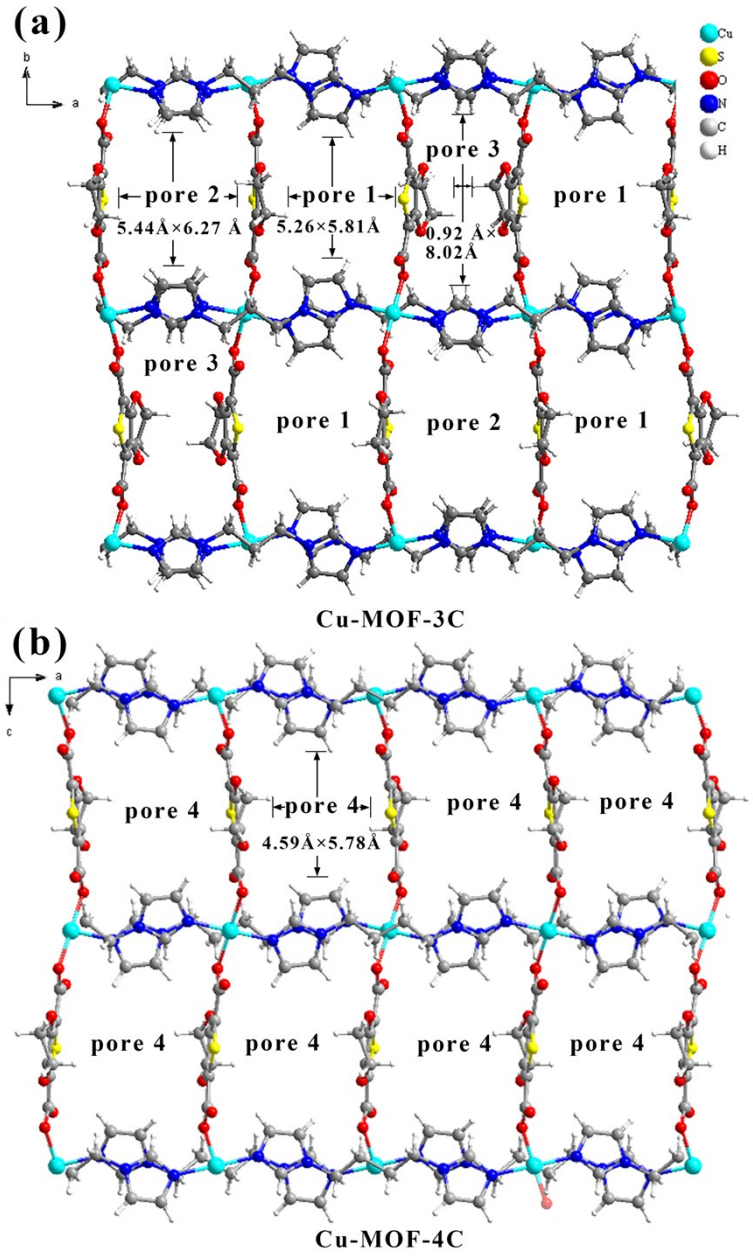

Fig. S4 The interlayer pores of (a) Cu-MOF-3C and Cu-MOF-4C.

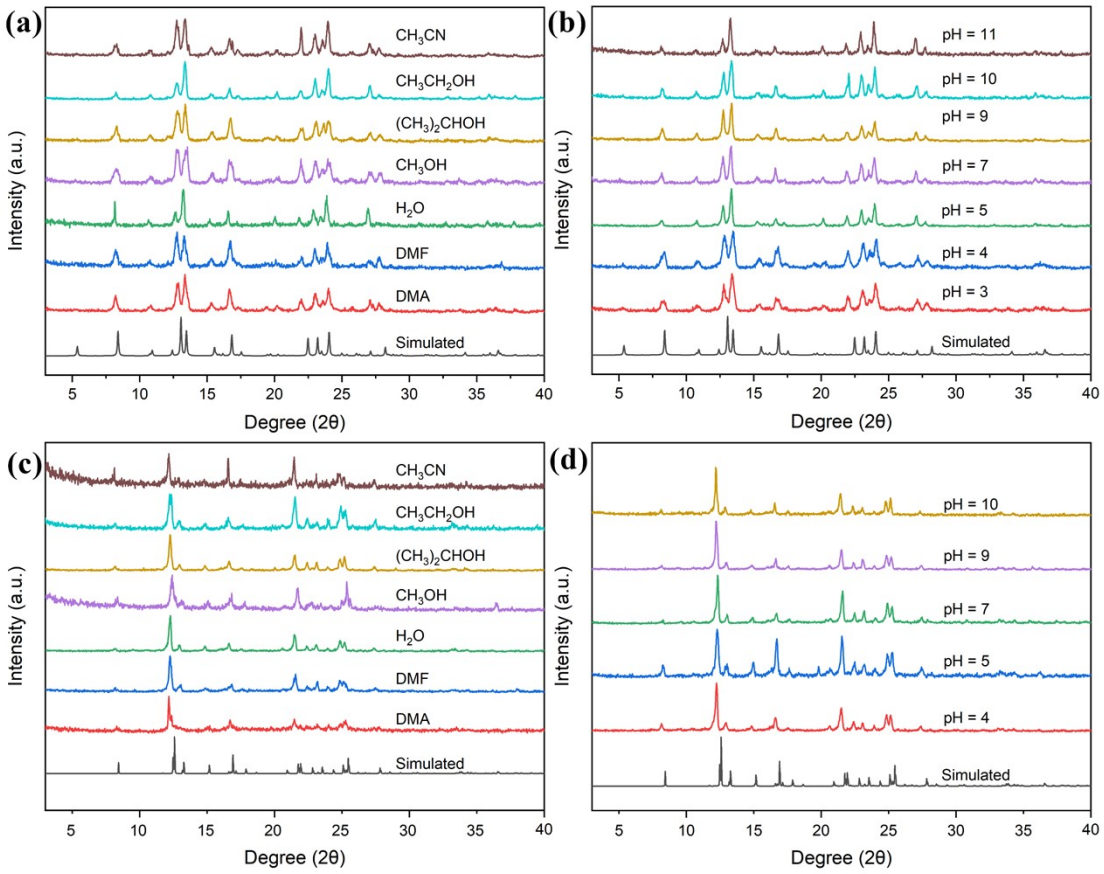

Fig. S5 PXRD patterns of Cu-MOF-3C immersing in different (a) solvent and (b) pH of water for 24 h. PXRD patterns of Cu-MOF-4C immersing in different (c) solvent and (d) pH of water for 8 h.

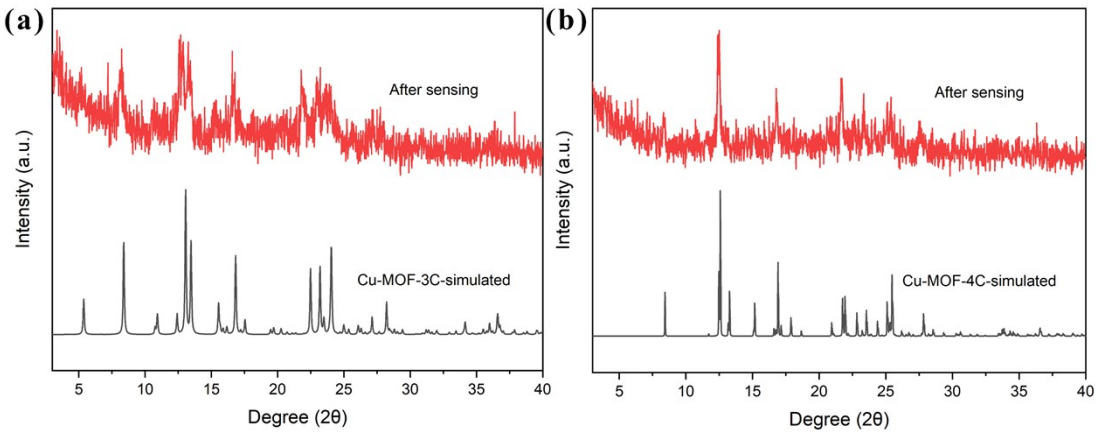

Fig. S6 PXRD patterns of (a) Cu-MOF-3C and (b) Cu-MOF-4C after CV measurement in PBS solution containing 200 μM dopamine.

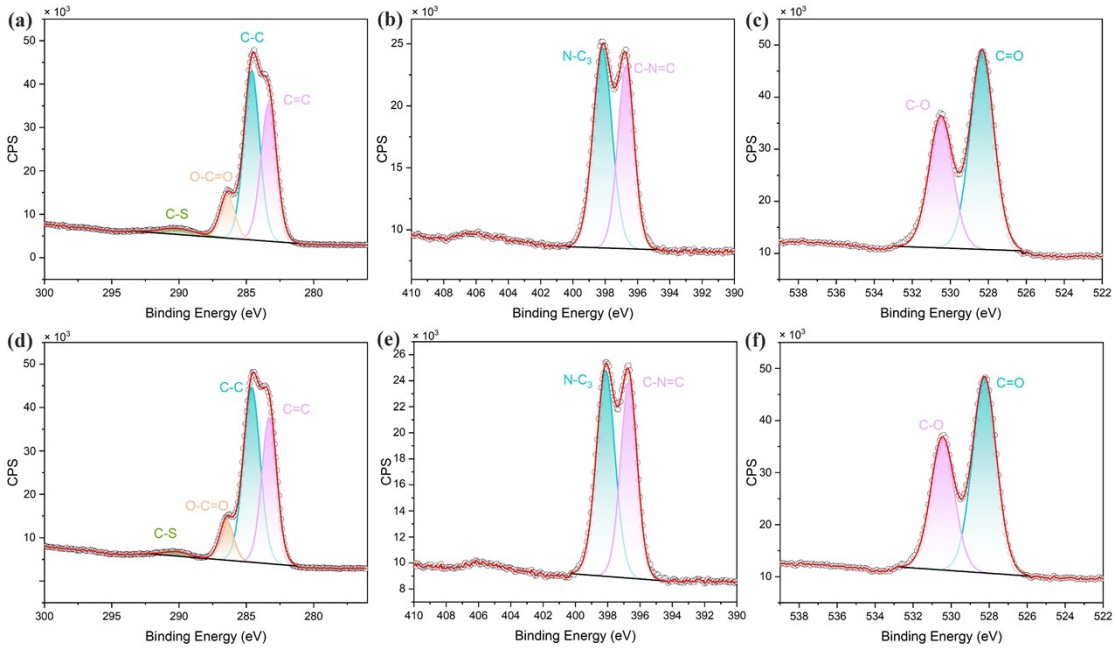

Fig. S7 High-resolution spectrums of (a) C 1s, (b) N 1s, (c) O 1s in Cu-MOF-3C and (d) C 1s, (e) N 1s, (f) O 1s in Cu-MOF-4C.

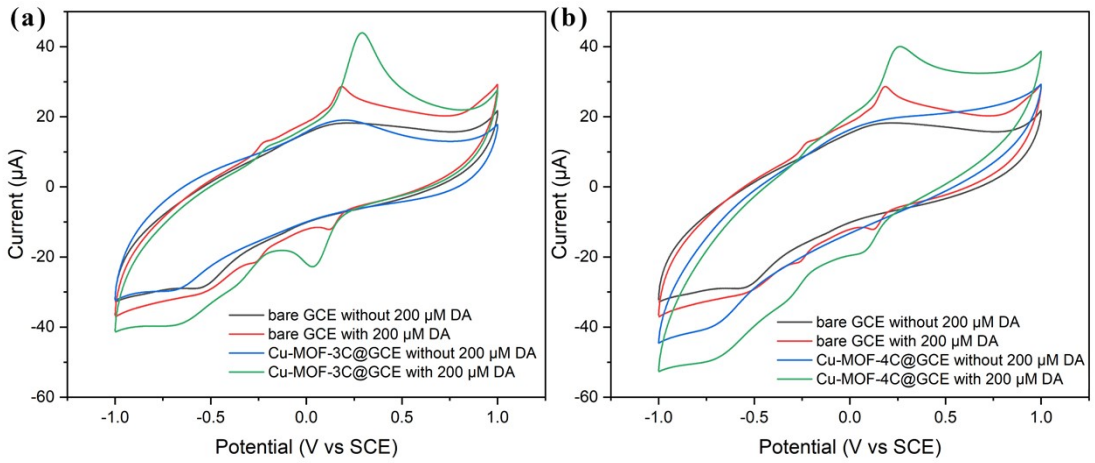

Fig. S8 CV curves of (a) Cu-MOF-3C@GCE and (b) Cu-MOF-4C@GCE and bare GCE in PBS with and without 200 μM DA.

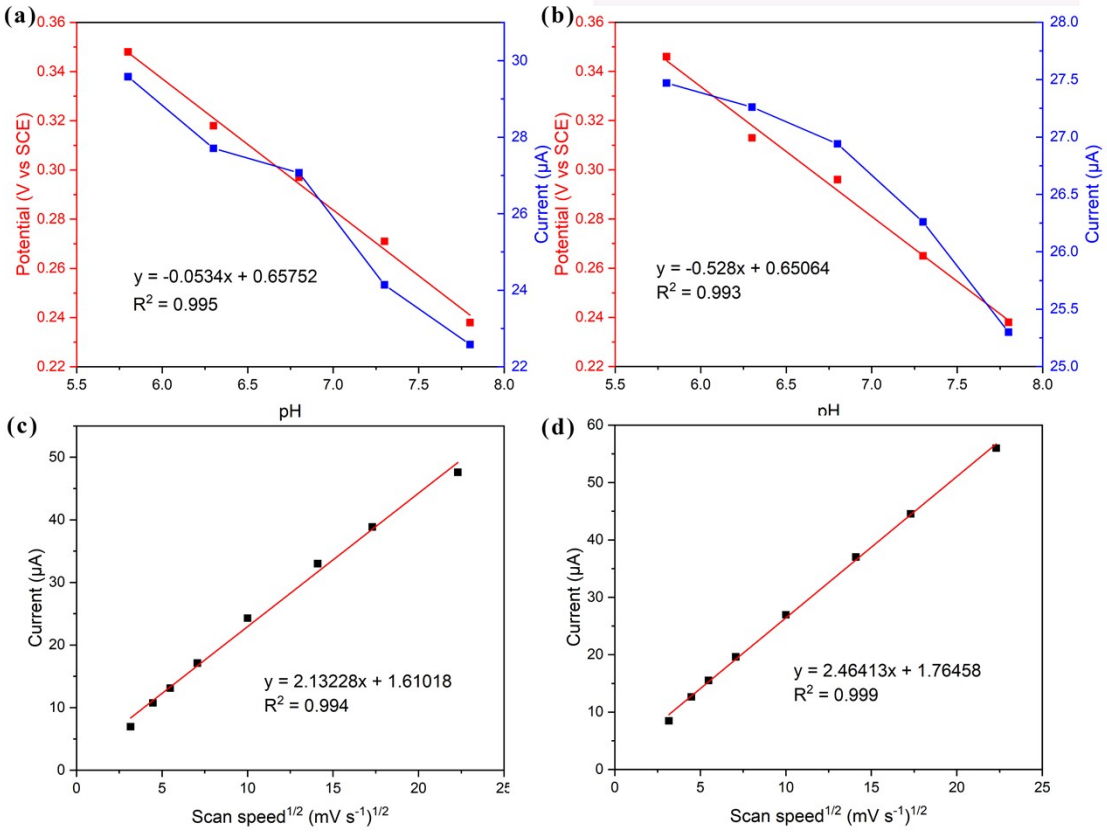

Fig. S9 Current and the liner plot between potential and pH of (a) Cu-MOF-3C and (b) Cu-MOF-4C. Linear relationship between peak current and the square root of scanning rates of (c) Cu-MOF-3C and (d) Cu-MOF-4C.

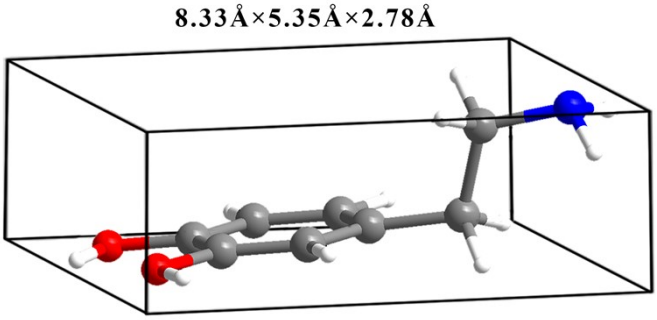

Fig. S10 Size of free dopamine molecule.

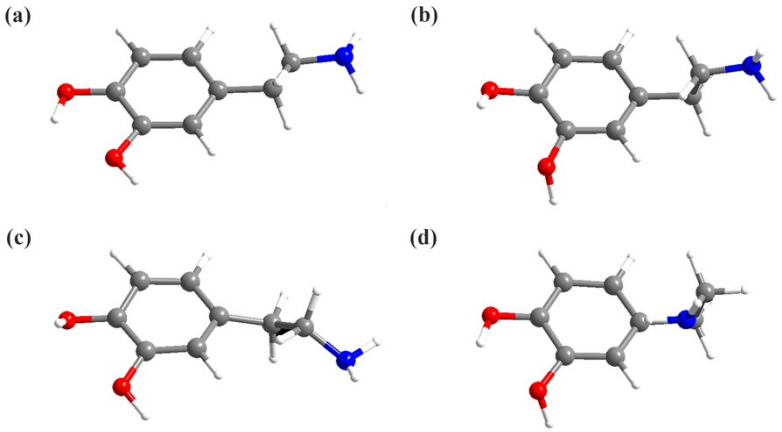

Fig. S11 The morphology of (a) free dopamine molecule and dopamine molecule in Cu-MOF-3C at (b) pore 1, (c) pore 2 and in Cu-MOF-4C at (d) pore 4.

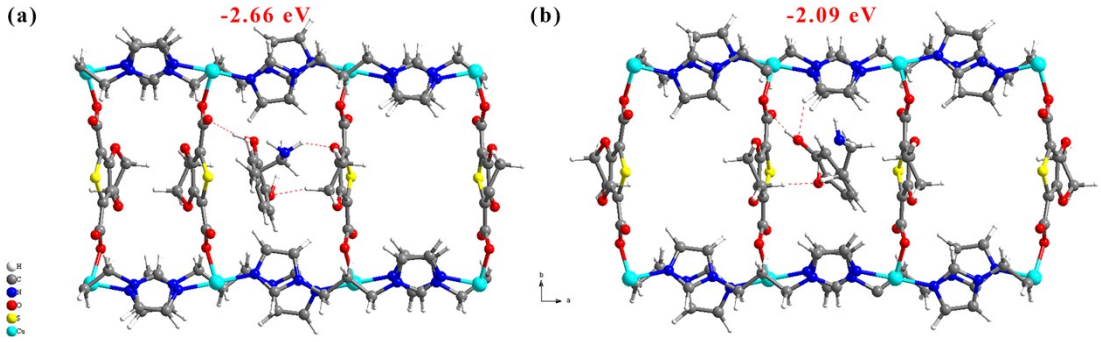

Fig. S12 DA binding sites for (a) pore 1 and (b) pore 2 in Cu-MOF-3C.

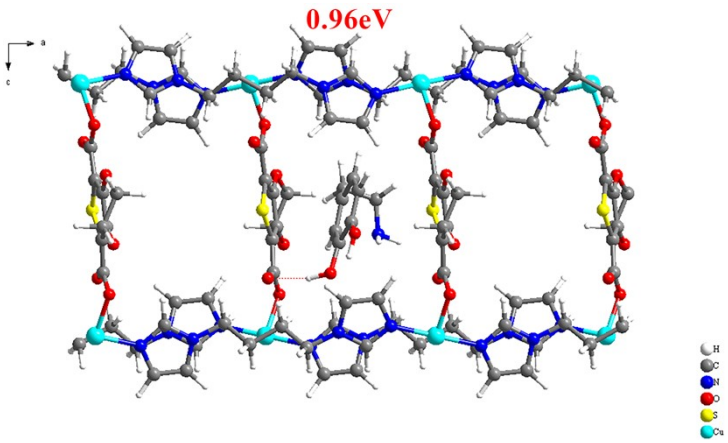

Fig. S13 DA binding site for pore 4 in Cu-MOF-4C.

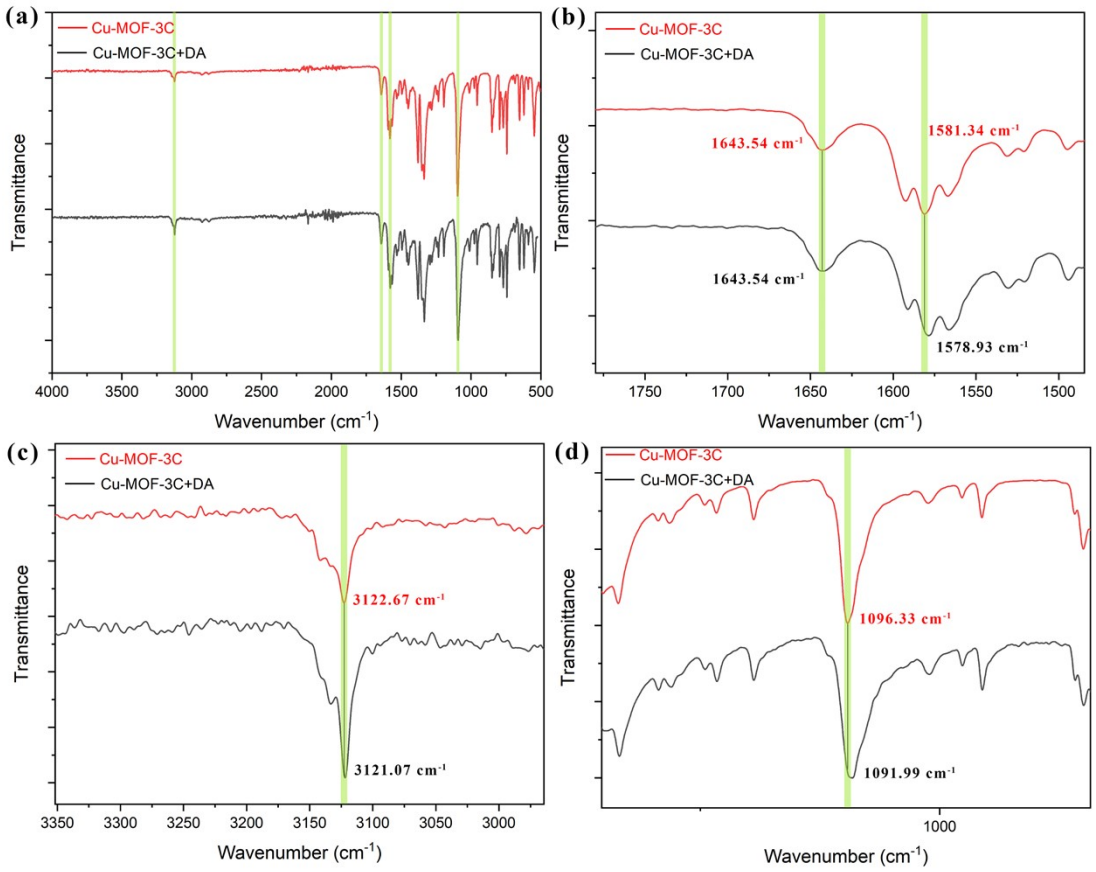

Fig. S14 (a) FT-IR images of Cu-MOF-3C before and after immersing in 10 mM DA solution for 8 h. Enlarged FT-IR images of Cu-MOF-3C at (b) 1581.34 cm^{-1}, (c) 3122.67cm^{-1} and (d) 1096.33 cm^{-1}.

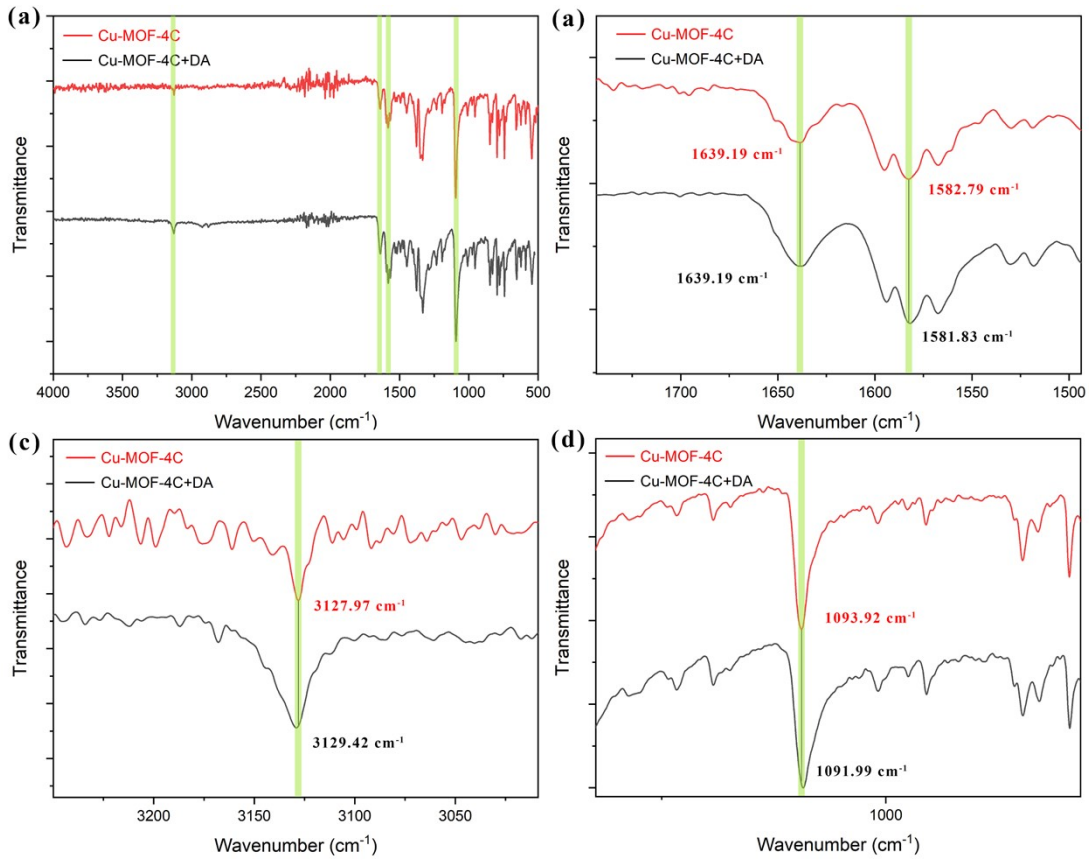

Fig. S15 (a) FT-IR images of Cu-MOF-4C before and after immersing in 10 mM DA solution for 8 h. Enlarged FT-IR images of Cu-MOF-4C at (b) 1582.79 cm^{-1}, (c) 3127.97cm^{-1} and (d) 1093.92 cm^{-1}.

Table S1: Crystal data and parameter of Cu-MOF-3C and Cu-MOF-4C.

	Cu-MOF-3C	Cu-MOF-4C
Empirical formula	$C_{38}H_{41}Cu_2N_9O_{13}S_2$	$C_{22}H_{27}CuN_5O_7S$
Formula weight	1023.00	569.08
CCDC number	2487980	2487981
Temperature/K	140.88(10)	80.0(2)
Crystal system	orthorhombic	orthorhombic
Space group	$Pna2_1$	$Pna2_1$
a/Å	26.1953(12)	14.1789(3)
b/Å	21.0514(8)	8.09640(10)
c/Å	7.9877(4)	20.9557(3)
α/°	90	90
β/°	90	90
γ/°	90	90
Volume/Å^3	4404.8(3)	2405.67(7)
Z	4	4
ρcalcg/cm^3	1.543	1.571
μ/mm^{-1}	2.709	2.565
F(000)	2104.0	1180.0
Crystal size/mm^3	0.04 × 0.04 × 0.005	0.04 × 0.02 × 0.005
Radiation	Cu Kα (λ = 1.54184)	Cu Kα (λ = 1.54184)
2Θ range for data collection/°	6.748 to 153.67	8.438 to 153.01

Table S2: Comparison of auxiliary ligands and pore sizes in Cu-MOF-3C and Cu-MOF-4C.

		Cu-MOF-3C	Cu-MOF-4C	
Auxiliary ligand length	IMPP	9.26 Å	IMBT	10.48 Å
Intralayer pore size (2D)	pore A	8.63 Å×7.86 Å	Pore C	11.79 Å×5.78 Å
	pore B	12.78 Å×5.81 Å		
Interlayer pore size (3D)	Pore 1	5.26 Å×5.81 Å	Pore 4	4.59 Å×5.78 Å
	Pore 2	5.44 Å×6.27 Å		
	Pore 3	0.92 Å×8.02 Å		

Table S3: Comparison of detecting DA in different methods.

Materials	Liner range (μM)	LOD (μM)	Technique	Reference
CuNi-MOF@rGO	1-500	9.41	i-t	1
CuO/Cu_2O	2-20	0.388	i-t	2
MOF-235/GCE	10-90	3.33	DPV	3
CeO_2/siloxene/GCE	0.292–7.8	0.292	DPV	4
SO_3-MOF-808/GO	50-500	2.3	DPV	5
tyrosinase/NiO@ITO	2-500	1.038	CV	6
5-PLA/COP	2-7	1.7	CV	7
SPCE-Fe_3O_4/SPEEK	5-50	7.1	SWV	8
FeS_2/CoS_2NHs/GCE	1-24000	1.1	LSV	9
TM-CNT600	10.7–24.2	1.42	LSV	10
Cu-MOF-3C@GCE	0.5-500	0.48	DPV	This work
Cu-MOF-4C@GCE	2-300	1.32	DPV	This work

References:

1. C. Wang, Y. Zhang, Y. Liu, X. Zeng, C. Jin, D. Huo, J. Hou and C. Hou, *Anal. Chim. Acta*, 2024, **1299**, 342441.

2. R. Mondal, B. Show, S. F. Ahmed and N. Mukherjee, *Bull. Mater. Sci.*, 2024, **47**, 62.

3. K. Liu, Y. Chen, X. Dong and H. Huang, *Inorg. Chem. Commun.*, 2022, **142**, 109584.

4. C. Ge, R. Ramachandran and F. Wang, *Sensors*, 2020, **20**, 4880.

5. C.-H. Shen, Y.-N. Chang, Y.-L. Chen and C.-W. Kung, *ACS Materials Letters*, 2023, **5**, 1938-1943.

6. A. Roychoudhury, S. Basu and S. K. Jha, *Biosens. Bioelectron.*, 2016, **84**, 72-81.

7. N. Borras, A. Sánchez-Sanz, J. Sans, F. Estrany, M. M. Pérez-Madrigal and C. Alemán, *Eur. Polym. J.*, 2023, **187**, 111915.

8. M. N. Ranku, G. E. Uwaya and O. E. Fayemi, *Molecules*, 2021, **26**, 5357.

9. Z. Zhao and L. Zheng, *J. Electroanal. Chem.*, 2024, **956**, 118101.

10. V. B. Jaryal, S. Kumar, D. Singh and N. Gupta, *ChemNanoMat*, 2024, **10**, e202300637.